Mon. Not. R. Astron. Soc. **386,** 2031–2038 (2008) doi:10.1111/j.1365-2966.2008.13146.x

Asteroids on Earth-like orbits and their origin

R. Brasser[1⋆] and P. Wiegert[2⋆]

[1]*Department of Physical and Environmental Science, University of Toronto at Scarborough, Toronto, ON, Canada*
[2]*Department of Physics & Astronomy, The University of Western Ontario, London, ON, Canada*

Accepted 2008 February 22. Received 2008 February 5; in original form 2007 July 12

ABSTRACT

The orbit of 1991 VG and a set of other asteroids whose orbits are very similar to that of the Earth have been examined. Its origin has been speculated to be a returning spacecraft, lunar ejecta or a low-inclination Amor- or Apollo-class object. The latter is arguably the more likely source, which has been investigated here. The impact probability for these objects has been calculated, and while it is larger than that of a typical near-Earth asteroid (NEA), it is still less than 1:200 000 over the next 5000 yr. In addition, the probability of an NEA ever ending up on an Earth-like orbit has been obtained from numerical simulations and turned out to be about 1:20 000, making this a rare class of objects. The typical time spent in this state is about 10 000 yr, much less than the typical NEA lifetime of 10 Myr.

Key words: minor planets, asteroids – Solar system: general.

1 INTRODUCTION

In the autumn of 1991 J. V. Scotti reported a fast-moving object in the evening sky with the 0.91-m Spacewatch telescope (IAUC 5387). A computation of the orbit by Brian G. Marsden in that same circular resulted in an orbit strikingly similar to that of the Earth. The circular added that the osculating geocentric orbit had an eccentricity $e > 3$ and that therefore the object might be a returning spacecraft. This hypothesis was emphasized in IAUC 5402 in which short-period changes in brightness were observed. The light curve appeared as that of a rapidly rotating satellite with highly reflective panels. If an albedo of about 0.5 is assumed, the reflective area would be about 30 m^2, suggesting the origin to be a spacecraft. Computations of the orbit back in time showed that the object had another, but more distant encounter with the Earth in 1974–1975, i.e. one synodic period ago, and another in the late 1950s, both times consistent with a spacecraft launch. The spacecraft hypothesis was once again suggested for the origin of the object 2000 SG344,[1] an object of similar size than 1991 VG and also having an Earth-like orbit.

A few years later, Rabinowitz et al. (1993) reported an overabundance of small-Earth approachers or SEAs, of which 1991 VG is listed as a member, though a somewhat unusual one. Most of these SEAs have a diameter $d < 50$ m and are on low-eccentricity (e), low-inclination (i) orbits and semimajor axis (a) not too deviant from unity. The sample of SEAs led Rabinowitz et al. (1993) to suggest there is a near-Earth asteroid (NEA) belt, of which most members have not been detected yet. Subsequently Bottke et al. (1996) used a Monte Carlo method using Öpik's (1976) equations to understand what the source of these SEAs is and concluded that it is difficult to achieve an orbit similar to that of the Earth when the source is coming directly from asteroid belt. The best source, according to Bottke et al. (1996) are Amor-type fragments that evolve from low-eccentricity Mars-crossing orbits beyond the line $a(1 - e) = 1$ au. In an independent study, Gladman et al. (1997) show that some small fraction of asteroids in the ν_6 secular resonance can reach low-eccentricity orbits with $a \sim 1$ for a brief period in time, which is a different source from Bottke et al. (1996), paving the way for further study.

Even though Rabinowitz et al. (1993) and Bottke et al. (1996) mention 1991 VG as a member of the SEA group, there was no detailed study of its orbit after IAUC 5402 until Tancredi (1997), where its orbit was simulated for up to 2 Myr and several places of origin of the object were explored, including the returning spacecraft hypothesis. Tancredi (1997) showed that its motion is dominated by close approaches with the Earth, which occur every synodic period since both nodes are close to the Earth's orbit. From Tancredi's (1997) paper it is clear that no secular theory can be applied since the three angles longitude of the ascending nod (Ω), argument of pericentre (ω) and mean longitude (λ) vary chaotically; the three other variables a, e and i vary but keep the Tisserand parameter with respect to the Earth approximately constant. Due to the fact that the motion is dominated by close approaches with the Earth and that the two angles Ω and ω do not circulate, Tancredi (1997) noted that Öpik's (1976) equations cannot be used to compute the impact probability with the Earth. From the latter theory, the frequency of impact f should vary $\propto r^2$ where r is the geocentric distance. Instead, he found $f \propto r^{1.23}$ – caused by gravitational focusing – and an impact probability of $1/200\,000$ yr^{-1}, much larger than most NEAs (Chyba 1993). Yet, Tancredi's (1997) impact probability *is* similar to that found by Chyba (1993), who took the sample from Rabinowitz et al. (1993) and computed the probability of impacting

⋆E-mail: brasser_astro@yahoo.com (RB); pwiegert@uwo.ca (PW)
[1] http://science.nasa.gov/headlines/y2000/ast06nov_2.htm.

© 2008 The Authors. Journal compilation © 2008 RAS

Table 1. Heliocentric orbital elements for a selection of SEAs whose orbits are very similar to that of the Earth (co-orbital asteroids are excluded). The epoch is JD 245 3800.5. Elements are taken from the NeoDys web pages. $T_{\rm E}$ is the Tisserand parameter with respect to the Earth and $U = \sqrt{3 - T_{\rm E}}$ is the encounter velocity with respect to the Earth. H is the absolute magnitude and the last column is a computed diameter, assuming an albedo in the 15 per cent range (see text).

Object	a (au)	e	i (°)	Ω (°)	ω (°)	M (°)	$T_{\rm E}$	U	H	Diameter (m)
1991 VG	1.026 83	0.049 21	1.446	73.97	24.475	227.141	2.997	0.051	28.4	8.4
2000 SG344	0.977 397	0.066 95	0.11	192.225	274.924	132.351	2.996	0.064	24.8	44
2006 QQ56	0.986 803	0.046 08	2.796	161.458	330.541	270.547	2.995	0.066	25.9	26
2001 GP2	1.037 83	0.073 972	1.279	196.888	111.273	130.082	2.995	0.071	26.9	17
2007 VU6	0.974 697	0.091 113	1.200	224.417	32.837	129.509	2.998	0.090	26.6	19
2001 FR85	0.982 723	0.027 937	5.244	183.099	233.566	150.214	2.991	0.094	24.5	50
2006 BZ147	1.023 19	0.099 252	1.425	140.676	95.679	297.214	2.990	0.100	25.4	33
2006 DQ14	1.026 77	0.053 561	6.328	155.54	291.844	71.495	2.985	0.121	27.0	39
2007 XB23	0.982 978	0.028 853	8.451	260.885	84.006	44.731	2.978	0.149	27.1	15
2002 PN	1.014 28	0.068 915	9.145	309.54	107.381	87.344	2.969	0.174	24.8	44
2007 UP6	0.968 503	0.094 359	9.592	31.575	236.484	117.82	2.965	0.188	22.9	105
2006 JY26	0.981 613	0.086 923	1.977	47.119	296.765	188.499	2.911	0.298	28.3	8.5
2005 CN61	0.990 768	0.068 728	9.535	147.106	249.085	125.815	2.904	0.310	25.3	35

the Earth using Öpik's (1976) method. Chyba (1993) does note that Öpik's method does not work well for low-inclination objects and subsequently excludes 1991 VG from his future computations. The impact velocity for 1991 VG is close to the escape velocity at the Earth's surface so that the relative velocity between 1991 VG and the Earth is close to zero (see Table 1).

Apart from Tancredi (1997) there has not been a detailed study of the orbit of 1991 VG and the speculation to its origin and its high impact probability remain. The fact that there might be more asteroids with similar orbits have motivated the authors to search for objects on Earth-like orbits and that exhibit the same sort of motion dominated by close approaches with the Earth. The aim of this study is to briefly revisit the orbit of 1991 VG and a handful of objects on very similar orbits, to determine their origin in more detail through the use of numerical simulations and to compare this to the currently known NEA population.

This paper is divided as follows. Section 2 lists additional asteroids whose orbits are similar to that of the Earth. Section 3 contains our numerical methods. In Section 4 contains an overview of the motion of these asteroids. In Section 5 the impact probability of these objects is computed through numerical simulation of the orbits and clones. Section 6 deals with the origin of these objects. The summary and conclusions follow in Section 7.

2 1991VG'S COMPANIONS

The list of objects with orbits similar to that of the Earth including 1991 VG is given in Table 1. The elements are from the NeoDys[2] web pages. The criteria used to obtain these objects is as follows: $a \in [0.95, 1.05]$ au, $e \in [0, 0.1]$ and $i \in [0, 10^\circ]$. The quantity T is the Tisserand parameter with respect to the Earth, and is given by

$$T_{\rm E} = \left(\frac{1\,{\rm au}}{a}\right) + 2\sqrt{\left(\frac{a}{1\,{\rm au}}\right)(1-e^2)}\cos i. \quad (1)$$

The value U is the dimensionless encounter velocity with respect to the Earth at infinity, i.e. $U = v_{\rm r}/v_{\rm E}$ where $v_{\rm r}$ is the relative velocity between the asteroid and the Earth, and $v_{\rm E}$ is the circular velocity of the Earth at 1 au. It is only defined for crossing orbits and is related to the Tisserand parameter as $U = \sqrt{3 - T_{\rm E}}$. The quantity H is the absolute magnitude obtained from the NeoDys web pages and the last column lists an estimated diameter using the formula $\log(D/1\,{\rm m}) = 6.6 - 0.2H$, which is an intermediate formula obtained from the table at the MPC web pages,[3] and assumes an albedo of about 10–15 per cent. It has been suggested to us by the reviewer Gonzalo Tancredi to use the selection criterion $U \leqslant 0.1$ or $U \leqslant 0.15$ instead of the restrictions in a, e and i mentioned above. Using his selection has the unfortunate side effect of including some objects on distinctly non-Earth like orbits. Examples are 2001 BB16 ($a = 0.854,\ e = 0.172,\ i = 2\overset{\circ}{.}206; U = 0.097$) and 1998 KY26 ($a = 1.232,\ e = 0.202,\ i = 1\overset{\circ}{.}481; U = 0.121$). Of course, there are also a few NEAs with $U \leqslant 0.1$ that are not included in our sample above whose orbits may appear somewhat Earth-like, e.g. 2007 UN12 ($a = 1.054,\ e = 0.064,\ i = 0\overset{\circ}{.}237; U = 0.045$). This is a trade-off that we decided to live with. From now on, any asteroid that has its semimajor axis, eccentricity and inclination in the above-mentioned ranges shall be referred to as being on an 'Earth-like orbit', similar to Tancredi (1997). The asteroid 2003 YN107, which also fits these criteria, was not added to the list because it is an Earth co-orbital (Brasser et al. 2004a).

Of the above objects, 2000 SG344 received special attention because there was originally found to be a 0.2 per cent chance for it to impact the Earth in AD 2030 (Chodas & Chesley 2001). The last close approach with the Earth was in 1971. Pre-discovery observations later ruled out a collision, but there remains a 0.01 per cent chance of a collision in the 2070s. Dynamical and collisional arguments also suggest an origin from within the Earth–Moon system similar to 1991 VG, and since its orbit is similar to both the Earth and 1991 VG, it might indeed be a space probe or rocket stage (Chodas & Chesley 2001). However, its relatively large diameter (44 m if an assumed albedo of ∼15 per cent) might rule this scenario out immediately; indeed, even if the assumed albedo is 50 per cent, the estimated diameter is still close to 20 m, which is large for a spacecraft that reached a heliocentric orbit.

All of the objects in the above list have close approaches with the Earth every synodic period. In Table 2 previous and future approaches to the Earth are listed, which happen approximately

[2] http://newton.dm.unipi.it/neodys/.

[3] http://cfa-www.harvard.edu/iau/lists/Sizes.html.

Table 2. Past and future close approaches between the objects in the studied sample and the Earth.

Object	Years of approach (AD)
1991 VG	1975, 1991, 2017, 2039
2000 SG344	1971, 2000, 2029, 2070
2001 FR85	1975, 2001, 2040, 2081
2001 GP2	1981, 2001, 2020, 2049
2002 PN	1961, 2001, 2050, 2085
2005 CN61	1946, 2005, 2067
2006 BZ147	1977, 2006, 2036, 2062
2006 DQ14	1978, 2006, 2031, 2052
2006 JY26	1972, 2006, 2074
2006 QQ56	1965, 2006, 2051, 2091
2007 UP6	1967, 1988, 2008, 2027, 2048
2007 VU6	1952, 1982, 2008, 2037, 2063
2007 XB23	1972, 2008, 2026, 2045, 2068

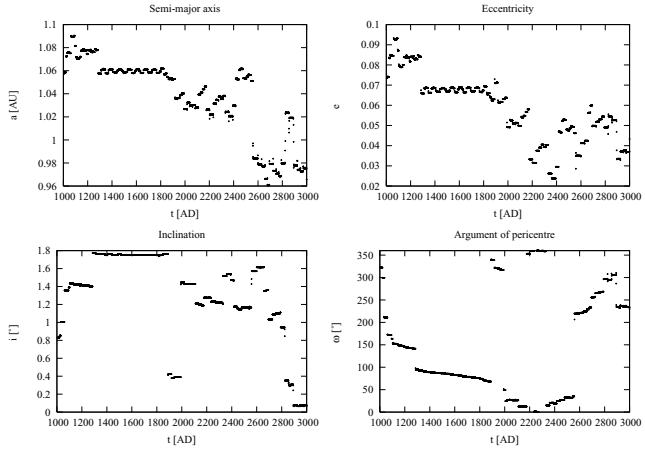

Figure 1. Several orbital elements versus time for 1991 VG from AD 1000 to 3000.

every synodic period. The intervals between close approaches with the Earth are too short in order for secular effects to change the orbit appreciably, so that, at least for the time being, the motion is entirely controlled by close approaches. Before the motion is studied in more detail, we digress for a moment to discuss our numerical and analytical methods employed.

3 NUMERICAL METHODS

Here we briefly discuss the numerical and analytical methods that have been employed during this paper.

For the purpose of this study, the orbits of 1991 VG and its companions have been cloned and numerically simulated forward in time. Backward computations have only been performed in a few cases. The cloning of the orbits of the objects in question was done according to the algorithm of Brasser et al. (2004b). The spread in the elements are computed using the covariance matrix $\mathbf{C}$ of the orbit, which is obtained from the NeoDys web pages. Denoting by $\boldsymbol{p}$ the vector containing the nominal orbital elements, the changes in the elements are

$$\Delta p_i = \xi_k \sqrt{\lambda_k} X_i^k, \tag{2}$$

where ξ_k is a random number with a Gaussian distribution, λ_k are the eigenvalues of the covariance matrix and the matrix X_i^k contains the latter's eigenvectors, and the summation index is k. For most orbits, the uncertainties are small, implying the orbits are quite well known. For most cases a hundred clones were used.

The bulk of the numerical simulations have been performed with the well-known RMVS3 integrator of the SWIFT package (Levison & Duncan 1994). The RMVS3 routine 'sniffs' for a close approach with a planet about 3.5 Hill radii ($3.5R_{\rm H}$) away, which sets an upper limit to the time-step that can be taken. For the Earth $R_{\rm H} \approx 0.01$ au so that the time-step cannot be larger than approximately $t \approx 3.5R_{\rm H}/v_{\rm E} \approx 2.03$ d. The authors settled for a time-step of 4×10^{-3} yr or 1.46 d. Since SWIFT does not document close approaches, many of the orbits were recomputed with a different symplectic, Wisdom–Holman integrator (Wisdom & Holman 1991) which handles close encounters by the Chambers method (Chambers 1999) to monitor the closest approach distance to the Earth. Simulations were run on an Intel C2Q machine and on the University of Toronto's 8-CPU Astrogrid beowulf cluster (AMD Opterons). Data analysis was done with SWIFTVIS.[4]

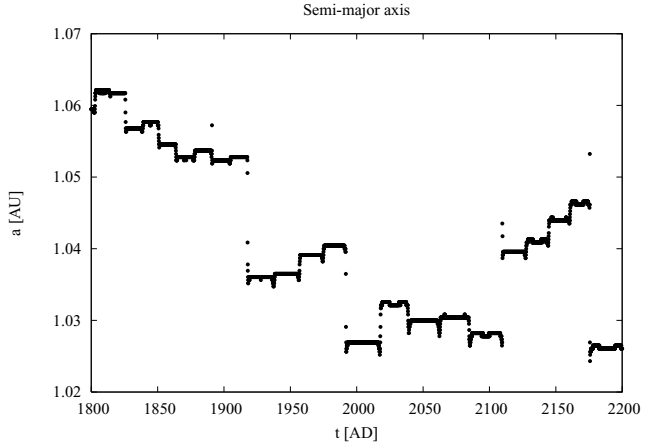

Figure 2. Semimajor axis of 1991 VG from AD 1800 to 2200. The kicks every synodic period are clearly visible.

Now we are ready to give a general overview of the orbits.

4 ORBIT PROPERTIES

Fig. 1 displays the time variation of four orbital elements (a, e, i, ω) as a function of time between AD 1000 and 3000 for 1991 VG. The chaotic, stochastic nature of the variations in the elements with each approach to the Earth after a synodic period is clearly seen and similar to that found by Tancredi (1997). Fig. 2 is a zoom of the top left-hand panel of Fig. 1 from AD 1800 to 2200. The frequent close approaches to the Earth manifest themselves in the kicks in energy, and therefore in semimajor axis. All the other objects in the sample experience the same behaviour, though the kicks are generally smaller. Fig. 3 displays the evolution in semimajor axis for 1991 VG and some clones, for 250 yr. One can see that after about 100 yr, around AD 2100, the orbits diverge quickly because of a very close approach with the Earth. These frequent close approaches are a source of chaos (e.g. Tancredi 1998) and a typical Lyapunov time for these objects is about 10 yr, in accordance with Tancredi (1998) who

[4] http://www.cs.trinity.edu/∼mlewis/SwiftVis/.

© 2008 The Authors. Journal compilation © 2008 RAS, MNRAS **386,** 2031–2038

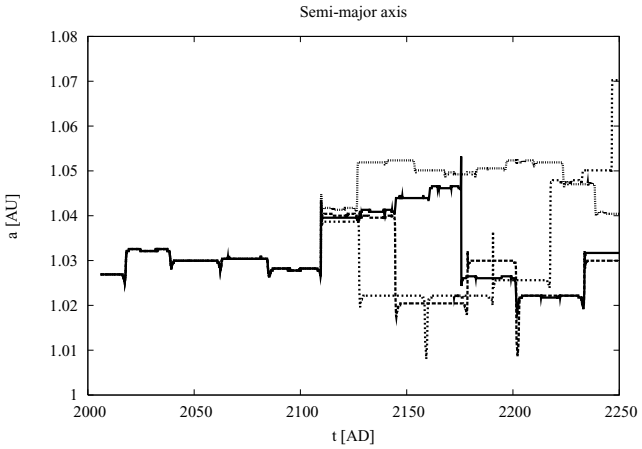

Figure 3. Semimajor axis of 1991 VG and some clones clearly displaying the divergent and chaotic behaviour of its orbit.

finds Lyapunov times of a few decades for objects with pericentre distance $q \sim 1$ au. In this particular case, the Lyapunov time is of the order of the synodic period of the object. Indeed, Tancredi (1998) finds that the most chaos comes from approaches to the planets at distances of a few Hill radii. Our results show that typical approach distances of the sample of asteroids studied is about 5 Hill radii and that the process is essentially a random walk in energy (Tancredi 1997). We found the typical rms energy change per Earth encounter for all objects in the sample to be $\Delta(1/a) = 3.5 \times 10^{-3}\,\mathrm{au}^{-1}$. The corresponding diffusion time to random-walk about 0.1 au^{-1} (since $a \in [0.95, 1.05]$) is then

$$t_\mathrm{d} = P_\mathrm{s}(1/a)\left[\frac{0.1\,\mathrm{au}}{\Delta\,(1/a)}\right]^2 \sim 10^4 \quad \mathrm{yr}, \tag{3}$$

where $P_\mathrm{s}(1/a)$ is the synodic period, for which we have taken 25 yr (corresponding to $a \sim 1.025$ au). So the Earth-like orbit state is very short lived. Given the very Earth-like orbits of these bodies, it is likely that their impact probability exceeds that of more typical NEAs, and is discussed in the next section.

5 IMPACT PROBABILITY

In this section we discuss the impact probability for each object. The impact probability scales with the approach distance as $f \propto d^2$ (Öpik 1976) but due to the nature of the motion, the exponent may be less than two: Tancredi (1997) showed it to be 1.23 for 1991 VG, implying the angles ω and Ω do not circulate, as he demonstrated, and that gravitational focusing plays a role.

We performed a 100-kyr long simulation of 200 clones of each object. We then counted the number of objects impacting the Earth. Since the orbits change appreciably on the order of 10–100 kyr, the impact rates will not be the same during the 100 kyr simulation. We therefore chose to compute the impact rate at various times during the simulation.

The results are given in Table 3. The values P_1 to P_3 are computed at 2 kyr – to compare with Chyba (1993) and Tancredi (1997) – 50 and 100 kyr. Instead of counting the total number of impacts over the time-span and then averaging, we computed the impact probability by the number of impacts occurring between the two times at which it was computed, i.e. the impact rate computed at 50 kyr is computed by the number of impacts occurring between 2 and 50 kyr. This was done to better take the orbital changes into account. The value of P_1 for 1991 VG is different from that of Chyba (1993) and Tancredi (1997) but still in the range of the error bars. The large uncertainties in the first column are caused by the small number of impacts recorded in that time. In order to improve statistics, another set of runs was done for 5000 yr with 2000 clones for each object in order to better compute the short-term impact rate. This is given in Table 4 and in the case of 1991 VG our value agrees with Chyba (1993) ($42.1 \times 10^{-7}\,\mathrm{yr}^{-1}$) and Tancredi (1997) ($50 \times 10^{-7}\,\mathrm{yr}^{-1}$).

As is obvious, the average impact rate for most objects in our sample is much larger than that of the other SEAs investigated by Chyba (1993) and Rabinowitz et al. (1993), whose typical rate is $3 \times 10^{-8}\,\mathrm{yr}^{-1}$. For more typical NEAs with orbits significantly different from the Earth, a typical impact rate for km-sized bodies is $5 \times 10^{-9}\,\mathrm{yr}^{-1}$ (Steel 1993).

Table 3. Impact probabilities after 2, 50 and 100 kyr.

Object	$P_1(10^{-7}\,\mathrm{yr}^{-1})$	P_2	P_3
1991 VG	100 ± 50	21 ± 5	6 ± 2
2000 SG344	100 ± 50	17 ± 4	4 ± 2
2001 FR85	$<25 \pm 25$	3 ± 2	4 ± 2
2001 GP2	25 ± 25	7 ± 2	2 ± 1
2002 PN	$<25 \pm 25$	$<1 \pm 1$	1 ± 1
2005 CN61	$<25 \pm 25$	$<1 \pm 1$	1 ± 1
2006 BZ147	$<25 \pm 25$	1 ± 1	6 ± 2
2006 DQ14	$<25 \pm 25$	1 ± 1	1 ± 1
2006 JY26	$<25 \pm 25$	6 ± 2	1 ± 1
2006 QQ56	75 ± 25	17 ± 2	9 ± 3
2007 UP6	$<25 \pm 25$	$<1 \pm 1$	$<1 \pm 1$
2007 VU6	$<25 \pm 25$	4 ± 2	3 ± 1
2007 XB23	25 ± 25	19 ± 4	10 ± 3

Table 4. Impact probabilities after 5000 yr (should be compared with Table 3).

Object	$P_1(10^{-7}\,\mathrm{yr}^{-1})$
1991 VG	48 ± 7
2000 SG344	42 ± 6
2001 FR85	2 ± 1
2001 GP2	11 ± 3
2002 PN	$<1 \pm 1$
2005 CN61	$<1 \pm 1$
2006 BZ147	9 ± 3
2006 DQ14	2 ± 1
2006 JY26	2 ± 1
2006 QQ56	13 ± 3
2007 UP6	$<1 \pm 1$
2007 VU6	6 ± 2
2007 XB23	3 ± 1

6 ORIGIN

It has been speculated that 1991 VG might be a returning spacecraft because of its very Earth-like orbit and its peculiar spectrum, yet this hypothesis was rejected because it is unlikely that a heliocentric orbit was reached by a spacecraft with such a large projected area (Tancredi 1997). Another possibility is that 1991 VG and companions are lunar ejecta. Tancredi (1997) favours this as the most likely explanation because the alternative – dynamical evolution

from the asteroid belt – has a very low probability (Bottke et al. 1996; Gladman et al. 1997), even though Tancredi (1997) argues that the cratering event that spawned 1991 VG is very unlikely too. Let us examine this scenario in more detail. The following arguments are due to Brett Gladman (personal communication).

Current observational estimates on the number of NEAs with diameter of the order of 10 m range from 10^7 to about 5×10^7 (Brown et al. 2002; Ivanov et al. 2002; Bottke et al. 2005). Suppose that only 5–10 per cent of these are on low-eccentricity orbits (Rabinowitz 1994), then we have about 10^5 such objects. Suppose that these represent the 1991 VG population and are lunar ejecta. Using the aforementioned number and a conservative cumulative size distribution $\propto d^{-2}$, we expect about 10^{10} lunar ejecta of 3 cm (for a corresponding mass <300 g, typical for lunar meteorites). About 10–30 per cent reach the Earth over about 100 000 yr (Gladman et al. 1995). The average arrival rate of meteors >100 g is about 30 000 yr^{-1} (Halliday, Blackwell & Griffin 1989), meaning that over the about 100 000 yr storage of the Antarctic ice sheet the lunar meteorites' flux should be about equal to that of the chrondites. This is simply not the case: it is three orders of magnitude lower, suggesting that there has been no recent enough impact to produce ejecta the size of 1991 VG and larger. Additionally, an even simpler (and more powerful) argument is that if any one such large crater formed in the last 100 000 yr, it would excavate so much more material than other smaller craters over this time-scale that this one crater's ejecta should completely dominate the flux of lunar meteorites. CRE and petrologic studies can determine such source–crater pairings. In fact, almost all the lunar meteorites are unpaired (the only reasonable pairing is for a launch event 1 Myr ago; see Warren 1994), and thus there is no evidence for such a large event. Hence the lunar ejecta hypothesis can be rejected and the only remaining source is the NEA population. Bottke et al. (1996) showed that the SEA class of objects might originate from the asteroid belt. We propose to examine this result in more detail.

Bottke et al. (2000) compute the debiased distribution in semimajor axis, eccentricity and inclination of the NEA population – henceforth called 'the Bottke distributions'. These distributions have been reproduced in Fig. 4 based on 40 000 fictitious NEAs obtained from Bill Bottke. From these NEAs, the corresponding distributions in pericentre distance, Tisserand parameter with respect to Earth and encounter velocity with respect to Earth for crossing orbits only have been generated, and are depicted in Fig. 5. The abrupt end in

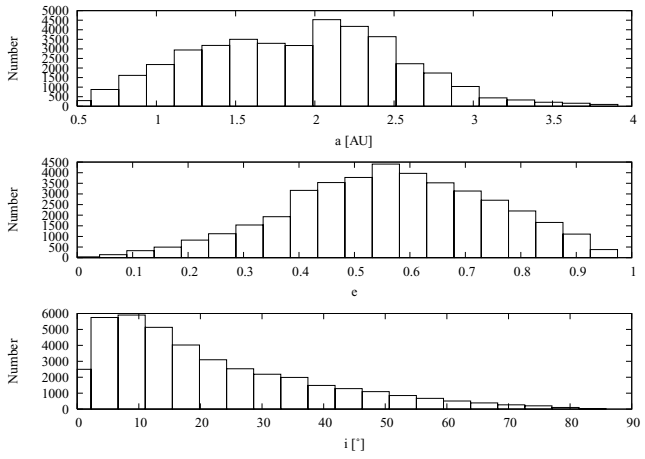

Figure 4. The unbiased distributions of semimajor axis, eccentricity and inclination of NEAs obtained from Bottke et al. (2000) (histograms) and our computed best fits (dashed lines).

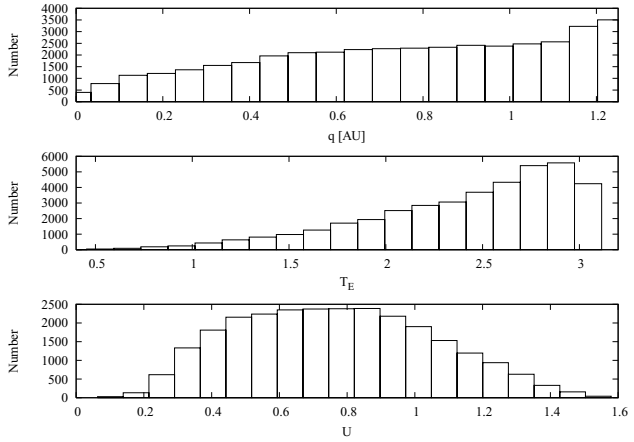

Figure 5. The distributions of pericentre distance, Tisserand parameter with respect to Earth, and encounter velocity with respect to Earth of NEAs generated from the unbiased semimajor axis, eccentricity and inclination distributions of Bottke et al. (2000).

the distribution of q beyond 1.3 au is an artefact of the generating programme, since it only takes NEAs with $q \leqslant 1.3$ au for now. The distribution in T_E peaks around 2.85 while the distribution in U is much broader. From the sample of fake NEAs in our possession, it was determined that the fraction of asteroids having $a \in [0.95, 1.05]$ au, $e \leqslant 0.1$ and $i \leqslant 10^\circ$ is $6.5 \pm 1 \times 10^{-5}$. Therefore, where do these 1991 VG-like asteroids originate from?

Bottke et al. (1996) find that the best sources for producing SEAs are low-eccentricity Amor-type asteroids. Many Earth-crossing asteroids have $U > 0.3$, as can be seen from Fig. 5. Since our sample of asteroids generally have $U < 0.1$, some mechanism must be responsible for reducing it. This can either be done by repeatedly passing an asteroid back and forth between the Earth and Venus, secular effects or by experiencing repeated close encounters with the Earth. These frequent Earth encounters increase the rms of the encounter velocity U but also increase its dispersion (Öpik 1976). Therefore, it is likely that our sample of asteroids are those few objects that are on the low-end tail of the distribution in U. This increase in the dispersion of U and the mechanism behind it is explained in the next subsection.

6.1 Randomization and acceleration

From Öpik's (1976) work encounters with the Earth have, besides the possibility for collision, three effects: to randomize the encounter velocity (i.e. to isotropize the directions) increase its rms value and increase its dispersion about the mean. The scattering angle, that is, the deflection experienced with each close encounter, will random walk until the total, vectorially added deflection equals 90°.

One can assign a cross-section for such a full angular deflection, $\pi\sigma$, which is a mathematical abstraction used to compute the total number of passages through the Earth's Hill sphere needed to randomize the encounter directions as well as compute the change in U with each such event (Öpik 1976). The radius at which to pass the Earth for randomization ($\sqrt{\sigma}/R_E$) or collision (s) is depicted in the top left-hand panel of Fig. 6. The top right-hand panel shows the number of encounters within the Hill sphere. The results of this figure have been obtained by numerical integration of Öpik's equations.

Since the Earth's orbit is not a circle, repeated encounters with the Earth will increase the mean value of U, $\langle U \rangle$, through random walk

© 2008 The Authors. Journal compilation © 2008 RAS, MNRAS **386,** 2031–2038

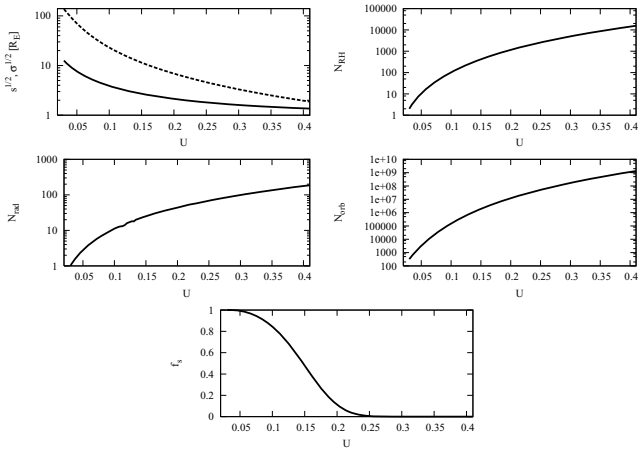

Figure 6. Encounter radius for randomization (upper line) or collision (lower line) (top left-hand panel), number of encounters through Hill sphere for randomization (top right-hand panel), number of randomizing encounters to reach current value of U starting at $U = 0.05$ (middle left-hand panel), and the number of orbits required to reach current value of U (middle right-hand panel) and the fraction of material surviving against collisions as a function of U (bottom panel).

(Öpik 1976). After a full randomization of encounter cross-section, i.e. once the total deflection reaches 90°, the additional mean-square encounter velocity is

$$\langle \Delta U^2 \rangle = \frac{\pi^2}{8} U_{\rm E}^2 \approx 3.0 \times 10^{-3}, \quad (4)$$

where $U_{\rm E}^2 = e_{\rm E}^2 + \sin^2 i_{\rm E}$ is the long-term average encounter velocity of the Earth relative to its circular standard. This increase in $\langle U \rangle$ decreases the cross-section for randomization and collision, as is obvious from the top left-hand panel of Fig. 6. One can subsequently compute how many orbits it takes to increase $\langle U \rangle$ by a certain amount and how many encounters with cross-section $\leqslant \pi\sigma$ are needed to accomplish this, which is depicted in the middle left-hand panel of Fig. 6 for a starting value of $\langle U \rangle = 0.05$, comparable to $U_{\rm E}$. This number of randomizing encounters, coupled with the average probability to have an encounter at said cross-section, yields the number of orbits needed to reach the desired value of $\langle U \rangle$ under the action of the Earth alone. This is displayed in the middle right-hand panel of Fig. 6. The reader should keep in mind that elimination through collision with the Earth occurs at a competing rate. The fraction of material surviving against collisions as a function of the value of $\langle U \rangle$ is plotted in the bottom panel of Fig. 6.

Assuming that repeated encounters with the Earth are responsible for placing asteroids on Earth-like orbits, then Fig. 6 suggests that only asteroids with $U < 0.2$ can end up temporarily on Earth-like orbits and not end up colliding with the Earth. Of course, the path to $U < 0.2$ can be through encounters or secular effects. Except 2002 PN, 2005 CN61, 2006 JY26 and 2007 UP6, which all have $U > 0.15$, the above analysis suggests that the remaining asteroids in our sample, all of which have $U < 0.15$, are objects that have had their values of U decreased significantly if they started off as NEAs with $U \geqslant 0.2$. However, the above analysis assumes that none have had an encounter with Venus or Mars to decrease their values of U with respect to the Earth. Simulations show that all objects diverge from their present orbits towards Venus or Mars, so that encounters with those planets in the past were likely. In the case of Mars, however, it is quite possible that those objects with larger values of U spent quite some time on an orbit with $q \sim 1$ and $a > 1$ but never suffered a close approach with Mars. Decreasing a and e while accelerating U increases the inclination, which might explain the high inclination of some of these objects. To summarize: the path towards Earth-like orbits is most likely one that involves decreasing U towards a value $U \lesssim 0.2$ through secular effects and encounters with the terrestrial planets, and a subsequent combination of secular effects and encounters with the Earth to generate a few objects with $U \lesssim 0.1$ This now needs to be checked through numerical simulations.

6.2 Numerical simulations and results

In order to verify the above hypothesis, several numerical simulations were performed. We took 64 000 asteroids from the Bottke distribution and simulated these for 1 Myr. Since the Bottke distribution represents a steady state and the median lifetime of an NEA is about 10 Myr (Gladman et al. 1997), the fraction of NEAs on Earth-like orbits throughout the 1-Myr simulation out of the total number of asteroids in the simulation should be approximately constant. From the set of simulations performed, the probability for an asteroid to enter the desired region was found to be $5.1 \pm 1.7 \times 10^{-5}$. This is in good agreement with the estimate given earlier. Fig. 7 shows the distribution of the original orbital elements, i.e. the elements at the start of the simulation derived from Bottke's distributions, for those fictitious NEAs that temporarily ended up on Earth-like orbits. The top left-hand panel of Fig. 7 shows the distribution in semimajor axis, the top right-hand panel is the eccentricity distribution; the bottom left-hand panel shows the distribution in pericentre and the remaining panel depicts the distribution in inclination. The majority of candidates have $a \sim 1$ au, $e \lesssim 0.3, i \lesssim 10^\circ$ and $q \sim 0.9$ au, which makes most objects Earth crossers. This particular configuration of orbital elements begs a little further investigation.

In order to explain the distributions of Fig. 7, we resort to a method first introduced by Kresák (1972). The top panel of Fig. 8 is a scatter plot in the $1/a - T_{\rm E}$ plane of those asteroids that temporarily had Earth-like orbits, while the bottom panel shows the dynamical path of a sample NEA in the same plane starting close to the ν_6 secular resonance, where a significant fraction of NEAs originate from (Bottke et al. 2000). The fat, solid line shows the criterion $e = 0$ for $i = 0$, so that above it no orbits are possible. The three fat, round dots show, from left- to right-hand side, the positions of Mars,

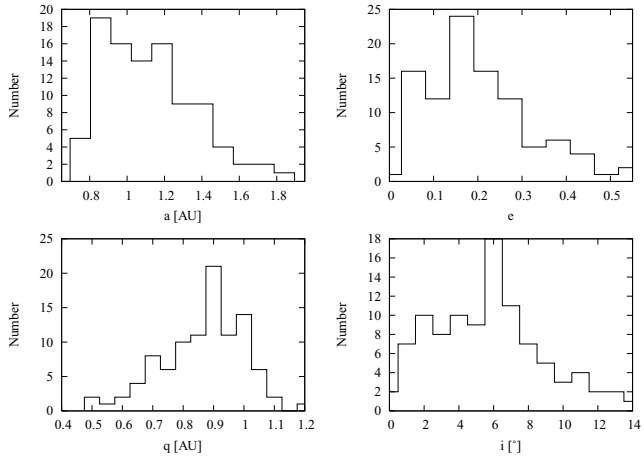

Figure 7. The distributions of original semimajor axis (top left-hand panel), eccentricity (top right-hand panel), inclination (bottom left-hand panel) and pericentre distance (bottom left-hand panel) of asteroids ever ending up on Earth-like orbits. Note how most orbits have $a \in (0.9, 1.2), e \sim 0.2, i \leqslant 10^\circ$ and $q \sim 0.9$.

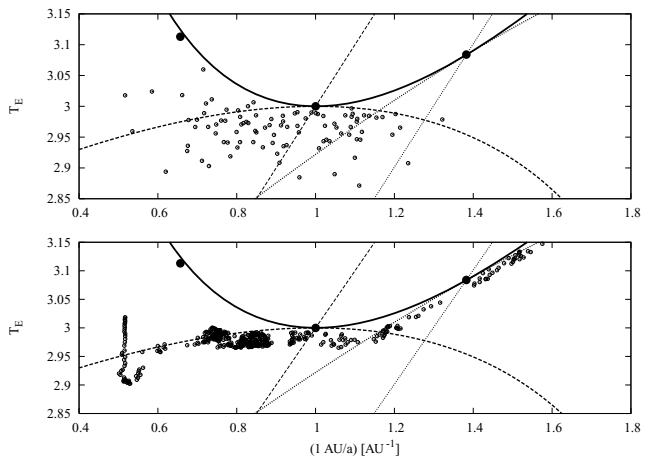

Figure 8. Top panel: position of starting conditions of fictitious NEAs that ever end up on Earth-like orbits in the $1/a$– $T_{\rm E}$ plane. The fat dots show the positions of Mars, Earth and Venus. Please see the text for a description of the various lines and their conditions. Bottom panel: evolution of a fictitious NEA in the $1/a$– $T_{\rm E}$ plane that is temporarily on an Earth-like orbit and ends up under the control of Venus.

Earth and Venus, respectively. The straight, dashed, upward-sloping line going through Earth's position at (1, 3) illustrates the criterion $\cos\theta = 0$, where $\cos\theta$ is given by (Öpik 1976)

$$2U\cos\theta = 1 - U^2 - \frac{1}{a}. \tag{5}$$

To the left-hand side of it, $\cos\theta > 0$ and the distribution in energy perturbations from the planet in consideration carry an excess in negative perturbations, i.e. the semimajor axis tends to decrease (Carusi, Valsecchi & Greenberg 1990). On the right-hand side of this line, the reverse is true and the semimajor axis tends to increase. The dotted, straight line going through Venus's position at (1.38, 3.08) depicts the $\cos\theta = 0$ criterion for Venus. The dashed, downward-sloping curve going through (1, 3) shows, for $i = 0$, orbits that are tangent to that of the Earth at either pericentre ($a > 1$) or apocentre ($a < 1$). The dotted curve going through (1.38, 3.08) illustrates the same criterion for Venus.

As is apparent from the top panel of Fig. 8, most candidates have $q < 1$ and most objects with $a > 1$ tend to have $\cos\theta > 0$, so that they are evolving towards the Earth. Similarly, those objects with $a < 1$ tend to have $\cos\theta < 0$ and are also evolving towards the Earth. A few objects start out being both Venus and Earth crossers. Please note that this particular configuration described above holds because $T_{\rm E}$ is close to 3 for the objects considered here. If, say, $T_{\rm E} = 2.6$ then orbits with $a > 1, q < 1$ and $\cos\theta < 0$ are possible and these objects tend to evolve away from the Earth.

The bottom panel of Fig. 8 shows the evolution of a fictitious NEA that temporarily resides on an Earth-like orbit. Since for Earth encounters the Tisserand parameter is approximately conserved, the evolution for Earth encounters tends to be along horizontal lines (see e.g. Valsecchi & Manara 1997). If Mars or Venus were to wrestle control of the object from the Earth, the evolution will subsequently proceed along straight lines parallel to the tangent to the circular limit at position of Mars or Venus. The object illustrated here starts close to the ν_6 secular resonance at $1/a \sim 0.5\,{\rm au}^{-1}$ and evolves straight down under the action of the resonance. Once the object passes the dashed, downward-sloping line, it becomes Earth crossing. Since it is situated to the left-hand side of the line $\cos\theta = 0$, the evolution proceeds be towards the Earth. It passes $a \sim 1$ with $T_{\rm E} \sim 2.97$. It evolves slightly further to the right through scattering at apocentre by the Earth towards a Venus-crossing orbit (dotted, curved line). At this point, Venus is able to take control of the object. Since at the first time of Venus crossing the object has $\cos\theta > 0$ with respect to Venus, it will evolve towards the orbit of Venus. This evolution, as can be seen, is along a straight line parallel to the tangent to the circular limit at the position of Venus. Since Venus controls the motion, the value of $T_{\rm E}$ is no longer conserved and ultimately the object no longer crosses the orbit of the Earth.

To recuperate: our results seem to suggest that objects that ever have Earth-like orbits come from low-inclination Apollo-type orbits, similar to Bottke et al. (1996), and the probability of an NEA to ever do so is of the order of 5×10^{-5}. Given that there are about 10^7 NEAs with sizes of about 10 m, we expect there to be a few hundred objects on Earth-like orbits. Current discovery rate appears to be a few per year, which is unsurprising given telescope efficiency, the long synodic periods and encounter conditions.

7 CONCLUSIONS

The dynamical evolution of the peculiar NEA 1991 VG has been investigated as well as that of several other bodies whose orbits are also very similar to that of the Earth. The motion can be adequately described as chaotic diffusion in energy along lines of constant Tisserand parameter. By computing the typical energy change per synodic period, a time can be computed on how long objects should exist on such orbits. This turns out to be of the order of 10 kyr: short compared to the typical lifespan of an NEA of 10 Myr (Gladman et al. 1997).

Secondly, the impact probability is computed for each object and tabulated at various epochs: 2, 50 and 100 kyr from now. In addition, a high-precision estimate over the first 5 kyr is given by using more test particles. Excepting 2002 PN, 2005 CN61 and 2007 UP6, all objects have impact probabilities much higher than a typical NEA, by up to two orders of magnitude. However, impact remains very unlikely for all objects considered.

Since one can most likely rule out spacecraft (Tancredi 1997) or lunar ejecta as the origin of these bodies, the most likely source is low-eccentricity Apollo and Amor asteroids (Bottke et al. 1996). These asteroids may have had their values of U lowered to $\sim$0.1 by passages close to the Earth. A large set of fictitious NEAs was generated from the Bottke distributions (Bottke et al. 2000) and simulated these for 1 Myr, from which it was found that the probability of an NEA ever ending up on an Earth-like orbit is about 5×10^{-5}.

Since the 1991 VG-like NEAs have orbits similar to Earth, they are only visible for a short time-span during their relatively long synodic periods. It is therefore likely that there exists a much larger population of these objects (Rabinowitz et al. 1993). Given the current estimate of NEAs with diameters about 10 m, it is expected there are a few hundred objects on Earth-like orbits.

ACKNOWLEDGMENTS

The authors wish to thank the reviewer, Gonzalo Tancredi, for constructive criticism in improving this manuscript. The authors express their sincerest gratitude to Bill Bottke for making available to us his source code and data files to generate fictitious Near-Earth Objects from his distributions. We also wish to thank Brett Gladman for his contributions to the lunar ejecta problem. Both RB and PW thank NSERC of Canada for funding this research. In addition, RB thanks CITA for partial funding through their National Fellowship programme.

© 2008 The Authors. Journal compilation © 2008 RAS, MNRAS **386,** 2031–2038

REFERENCES

Bottke W. F., Nolan M. C., Melosh H. J., Vickery A. M., Greenberg R., 1996, Icarus, 122, 406
Bottke W. F., Jedicke R., Morbidelli A., Petit J.-M., Gladman B., 2000, Sci, 288, 2190
Bottke W. F., Durda D. D., Nesvorný D., Jedicke R., Morbidelli A., Vokrouhlický D., Levison H. F., 2005, Icarus, 179, 63
Brasser R., Innanen K. A., Connors M., Veillet C., Wiegert P., Mikkola S., Chodas P. W., 2004a, Icarus, 171, 102
Brasser R., Mikkola S., Huang T.-Y., Wiegert P., Innanen K., 2004b, MNRAS, 347, 833
Brown P., Spalding R. E., ReVelle D. O., Tagliaferri E., Worden S. P., 2002, Nat, 420, 294
Carusi A., Valsecchi G. B., Greenberg R., 1990, Celest. Mech., 49, 111
Chambers J. E., 1999, MNRAS, 304, 793
Chodas P. W., Chesley S. R., 2001, BAAS, 33, 1196
Chyba C. F., 1993, Nat, 363, 701
Gladman B. J., Burns J. A., Duncan M. J., Levison H. F., 1995, Icarus, 118, 302
Gladman B. J. et al., 1997, Sci, 277, 197
Halliday I., Blackwell A. T., Griffin A. A., 1989, Meteoritics, 24, 173
Ivanov B. A., Neukum G., Bottke W. F., Hartmann W. K., 2002, in Bottke W. F., Cellino A., Paolicchi P., Binzel R. P., eds, Asteroids III. Univ. Arizona Press, Tucson, AZ
Kresák L., 1972, in Chebotarev G. A., Kazimiarchak-Polonskaya E. I., Marsden B. G., Reidel D., eds, The Motion, Evolution of Orbits, and Origin of Comets. Kluwer, Dordrecht
Levison H. F., Duncan M. J., 1994, Icarus, 108, 18
Öpik E. J., 1976, Interplanetary Encounters. Elsevier Scientific Publishing, Amsterdam
Rabinowitz D. L., 1994, Icarus, 111, 364
Rabinowitz D. L., Gehrels T., Scotti J. V., McMillan M. L., Wisniewski W., Larson S. M., Howell E. S., Mueller B. E. A., 1993, Nat, 363, 704
Steel D. I., 1993, MNRAS, 264, 813
Tancredi G., 1997, Celest. Mech. Dyn. Astron., 69, 119
Tancredi G., 1998, Celest. Mech. Dyn. Astron., 70, 181
Valsecchi G. B., Manara A., 1997, A&A, 323, 986
Warren P. H., 1994, Icarus, 111, 338
Wisdom J., Holman M., 1991, AJ, 102, 1528

This paper has been typeset from a TEX/LATEX file prepared by the author.